Clinical Chemistry 67:4
672–683 (2021)

A Highly Automated Mobile Laboratory for On-site Molecular Diagnostics in the COVID-19 Pandemic

Wanli Xing,[a,b,c,†] Jiadao Wang,[d,†] Chao Zhao,[e,†] Han Wang,[a,†] Liang Bai,[c] Liangbin Pan,[b,c] Hang Li,[b] Huili Wang,[a] Zhi Zhang,[b] Ying Lu,[a] Xiang Chen,[c] Sisi Shan,[f] Dong Wang,[b] Yifei Pan,[b] Ding Weng,[d] Xinying Zhou,[c] Rudan Huang,[b] Jianxing He,[g] Ronghua Jin,[h] Weimin Li,[i] Hong Shang,[j] Nanshan Zhong,[k] and Jing Cheng[a,b,*]

BACKGROUND: Infectious disease outbreaks such as the COVID-19 (coronavirus disease 2019) pandemic call for rapid response and complete screening of the suspected community population to identify potential carriers of pathogens. Central laboratories rely on time-consuming sample collection methods that are rarely available in resource-limited settings.

METHODS: We present a highly automated and fully integrated mobile laboratory for fast deployment in response to infectious disease outbreaks. The mobile laboratory was equipped with a 6-axis robot arm for automated oropharyngeal swab specimen collection; virus in the collected specimen was inactivated rapidly using an infrared heating module. Nucleic acid extraction and nested isothermal amplification were performed by a "sample in, answer out" laboratory-on-a-chip system, and the result was automatically reported by the onboard information platform. Each module was evaluated using pseudovirus or clinical samples.

RESULTS: The mobile laboratory was stand-alone and self-sustaining and capable of on-site specimen collection, inactivation, analysis, and reporting. The automated sampling robot arm achieved sampling efficiency comparable to manual collection. The collected samples were inactivated in as short as 12 min with efficiency comparable to a water bath without damage to nucleic acid integrity. The limit of detection of the integrated microfluidic nucleic acid analyzer reached 150 copies/mL within 45 min. Clinical evaluation of the onboard microfluidic nucleic acid analyzer demonstrated good consistency with reverse transcription quantitative PCR with a κ coefficient of 0.979.

CONCLUSIONS: The mobile laboratory provides a promising solution for fast deployment of medical diagnostic resources at critical junctions of infectious disease outbreaks and facilitates local containment of SARS-CoV-2 (severe acute respiratory syndrome coronavirus 2) transmission.

Introduction

The coronavirus disease 2019 (COVID-19) pandemic has posed major challenges to medical care globally (1–3). Timely diagnostics and treatment are critical in response to the COVID-19 pandemic (4). Among various diagnostic techniques, nucleic acid–based tests (NATs) of the causative agent, severe acute respiratory syndrome coronavirus 2 (SARS-CoV-2) (5, 6), including reverse transcription quantitative PCR (RT-qPCR) (7), reverse transcription loop-mediated isothermal amplification (LAMP) (8, 9), and reverse transcription recombinase polymerase amplification (10), have been vital in identifying potential virus carriers (11).

As large numbers of patients with respiratory infection go to medical centers for NATs, there is an accompanying high risk of cross-infection by SARS-CoV-2. For community screening, medical personnel are dispatched to collect specimens and send them to central laboratories for testing; such screening involves both tedious work and high risk of exposure. The inability to

[a]Department of Biomedical Engineering, School of Medicine, Tsinghua University, Beijing, China; [b]National Engineering Research Center for Beijing Biochip Technology, Beijing, China; [c]CapitalBio Technology, Beijing, China; [d]State Key Laboratory of Tribology, Tsinghua University, Beijing, China; [e]Department of Industrial Design, Academy of Arts & Design, Tsinghua University, Beijing, China; [f]Center for Global Health and Infectious Diseases, Comprehensive AIDS Research Center, Beijing, Advanced Innovation Center for Structural Biology, School of Medicine, Tsinghua University, Beijing, China; [g]State Key Laboratory of Respiratory Disease and National Clinical Research Center for Respiratory Disease, The First Affiliated Hospital of Guangzhou Medical University, Guangzhou, China; [h]Beijing Ditan Hospital, Capital Medical University, Beijing, China; [i]Department of Respiratory and Critical Care Medicine, West China Hospital, Sichuan University, Chengdu, China; [j]National Clinical Research Center for Laboratory Medicine, The First Affiliated Hospital of China Medical University, No 155, Nanjing North Street, Heping District, Shenyang, Liaoning Province, China; [k]State Key Laboratory of Respiratory Disease/National Clinical Research Center for Respiratory Disease/National Center for Respiratory Medicine/Guangzhou Institute of Respiratory Health/The First Affiliated Hospital of Guangzhou Medical University, Guangzhou, China.
*Address correspondence to this author at: Qinghuayuan 1# Beijing, Be, China.
Fax: 010-62773059; e-mails: weimin003@163.com, hongshang100@hotmail.com, nanshan@vip.163.com, jcheng@tsinghua.edu.cn
[†]Equal contribution.
Received November 28, 2020; accepted February 1, 2021.
DOI: 10.1093/clinchem/hvab027

inactivate the virus on-site may lead to biohazards due to unexpected leakage and contamination. For massive screening of travelers within a limited time at transportation hubs, on-site NATs are required. However, countries affected by the COVID-19 pandemic have had vast disparities in medical resources (12, 13). Especially in remote areas, NATs of the virus are largely unavailable given scarcity of medical centers with molecular diagnostics capability. The cost and time to build new stationary laboratories in the event of an outbreak are unsustainable. There is an urgent need to develop field-deployable fast-response mobile laboratories to provide on-site specimen collection and diagnostics.

Several field-deployable laboratories have been developed for on-site diagnostics. Early mobile laboratories adapted a room-based structure with specially designed equipment to improve portability (14–19). These laboratories required local housing and facilities such as water and electricity supply; owing to the need to establish separated working areas for nucleic acid amplification, their deployment suffered from poor mobility and dependence on local facilities. Later, truck-based mobile laboratories were developed with their own stand-alone power generators and ventilation systems that eliminated the need for local facilities; however, the large footprint restricted their use (20, 21).

We have previously developed a wide range of biochips and molecular diagnostic technologies based on laboratory-on-a-chip systems, including the pioneering bioelectronic chip that performed on-chip isolation, lysis, and hybridization of bacteria (22). More recently, we have focused on detection of infectious pathogens such as SARS-CoV-2 and *Mycobacterium tuberculosis* (23–26). In this article, we present a highly automated and fully integrated van-based mobile laboratory for rapid response to infectious disease outbreaks. The modular mobile laboratory is equipped with a 6-axis robot arm for automated oropharyngeal swab specimen collection, a heating module for quick pathogen inactivation, and a self-contained "sample in, answer out"–type microfluidic analyzer for nested isothermal amplification of pathogen nucleic acids. The results and laboratory status are monitored and automatically reported using an onboard information platform. Evaluation of the van-based mobile laboratory demonstrated excellent performance in specimen collection, inactivation, analysis, and reporting.

Materials and Methods

SYSTEM DESIGN

The mobile laboratory was constructed by remodeling a midsized van to achieve compact size and full functionality (see Fig. 1 and the online Data Supplement). Five discrete modules were developed and integrated to form the mobile laboratory, including automated specimen collection, quick specimen inactivation, pathogen NATs, a mobile laboratory information system, and a supporting system.

SPECIMEN COLLECTION

Manual collection of swab specimens from test participants is standard procedure; however, prolonged exposure to potential virus carriers and intensive labor have posed substantial risk to medical personnel (27). In the current work, a 6-axis robot arm was developed for automated specimen collection (Fig. 2, A). The specimen collection workflow is shown in Fig. 2, B. The robot arm was guided by streamed video images from a CCD camera with predetermined check positions for autocorrection. A tension and compression force sensor at 0.4-N resolution was integrated to provide force feedback and to reduce discomfort and potential harm to the test participant. Once the swab reached the oropharynx, the robot arm moved twice up and down and twice left and right, collecting a sufficient amount of oropharyngeal specimen for nucleic acid analysis.

To evaluate the efficiency of specimen collection, human cellular materials in oropharynx from healthy participants were collected and compared between automated collection by the robot arm and manual collection by trained medical personnel. The oropharyngeal cell samples were analyzed by LAMP using primers targeting human glyceraldehyde-3-phosphate dehydrogenase (*GAPDH*) gene. To assess the collected specimen, the time to positivity (Tp) value was determined as the second derivative inflection of amplification results, and lower Tp values indicated higher concentrations of the test sample (28). The Tp values of GAPDH curves were thus analyzed and compared between automated and manual collection.

PATHOGEN INACTIVATION

The collected specimen should be contained in a biosafety cabinet and inactivated before the NAT (29). Conventional water bath heating is time consuming and difficult to automate. A quick inactivation device was developed so that collected specimens were automatically loaded to the inactivation device inside the biosafety cabinet by the robot arm. The inactivation device utilized differential infrared radiation and thermoelectric effect to control the temperature in the upper and lower parts of the collection tubes, respectively (Fig. 3, A).

To measure temperature uniformity, a set of thermocouples were placed in the upper part of the collection tubes in each of the 16 positions of the holder. Temperature profiles by infrared radiation were captured in real time for the duration of 12 min at an interval of 10 s by a data-acquisition module (34972 A, Data Acquisition/Switch Unit; Keysight).

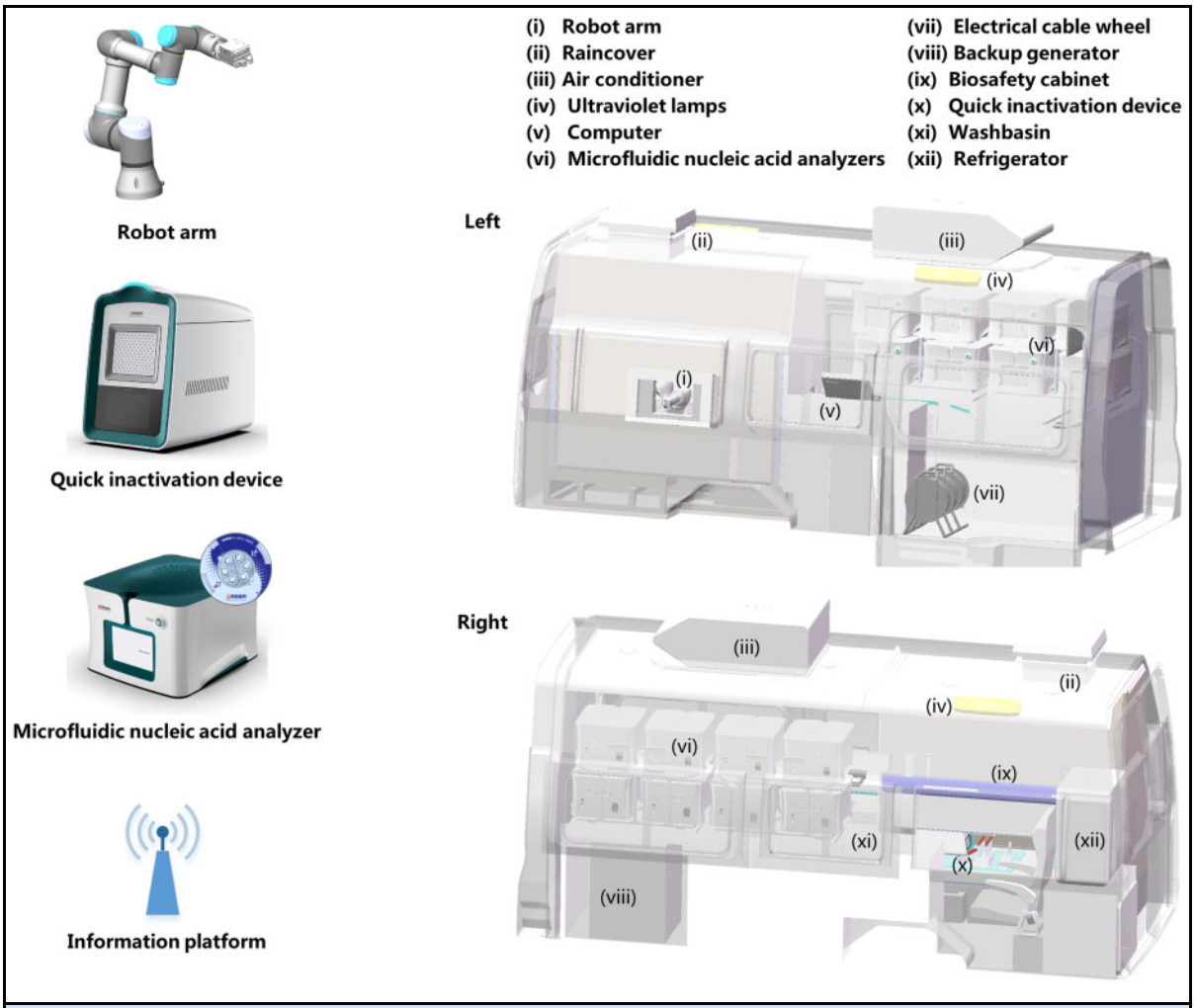

Fig. 1. Schematic illustration of the mobile laboratory. The mobile laboratory consists of the 6-axis robot arm; the quick pathogen-inactivation device; microfluidic nucleic acid analyzers; the information platform that automatically reports experimental results and laboratory status; the biosafety cabinet; and the supporting system, including separate ventilation systems, the electrical cable wheels, a backup generator, and the waterway system.

The quick inactivation device satisfied the needs of 2 working scenarios. On one hand, the collected specimen was maintained in preservation buffer, where both infrared bulbs and the Peltier element functioned as heaters for complete thermal inactivation. On the other hand, the collected specimen was maintained in lysis buffer, where infrared bulbs provided thermal inactivation of pathogen residues on the sidewalls and caps in the upper part, and the Peltier element remained idle for chemical inactivation of pathogens (30).

The inactivation efficiency was tested using the pseudoviruses Middle East respiratory syndrome coronavirus (MERS-CoV) and SARS-CoV-2. First, pseudovirus solutions were added to collection tubes at 200 μL and heated at 56 °C for 30 min or 70 °C for 12 min, respectively, with the Peltier element. Infrared radiation was applied simultaneously to the set temperature of 95 °C in the upper part of collection tubes. Viral activity of inactivated samples was examined using a luciferase assay (31). Second, smears of pseudovirus MERS-CoV were applied to upper sidewalls and caps of collection tubes and heated by infrared radiation to set temperatures of 90 °C, 95 °C, and 100 °C, respectively, whereas the lower part filled with 60 μL diethyl pyrocarbonate–treated water was not heated. For each temperature, infrared heating was tested for the duration of 5 min and 12 min, respectively. After quick inactivation, the tubes were vigorously shaken so that smears were remixed

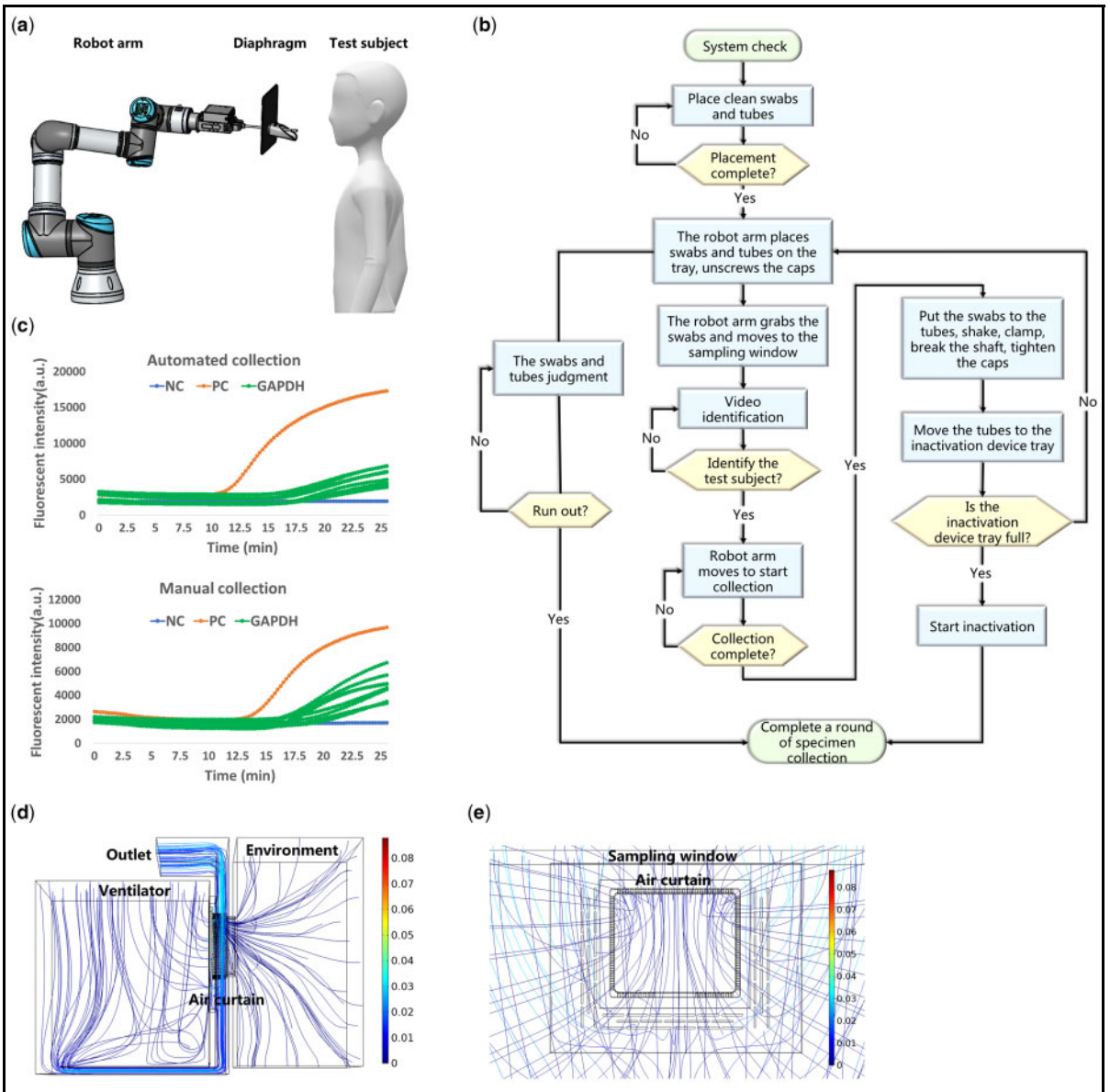

Fig. 2. Specimen collection system with the robot arm. (A), Schematic illustration of the specimen collection module. The robot arm sat behind a disposable diaphragm placed in front of the sampling window, where the test participant bit tightly on the diaphragm to allow wide opening of the mouth. (B), Workflow for specimen collection. (C), Comparison of collected human cellular specimen in oropharynx between the robot arm and the trained medical personnel. The green amplification curves indicate successful detection of the *GAPDH* gene from human cells ($n = 8$). Positive control (PC): duck plaque virus; negative control (NC): diethyl pyrocarbonate (DEPC)-treated water; internal quality control (IC): GAPDH. (D), Side view of the simulated profile of air flow in the biosafety cabinet. The speed of inlet air from the ventilator was 0.365 m/s, and the speed of air from the environment was 0.00365 m/s. The color bar indicates the speed of air flow. (E), Detailed view of the air flow profile near the air curtain of the sampling window. The color bar indicates the speed of air flow.

with diethyl pyrocarbonate–treated water for the luciferase assay. Considering that these pseudoviruses could infect host cells for only a single time and that the poor capability of infection may lead to false-negative results, the replicable vesicular stomatitis virus was utilized to simulate inactivation of real pathogens.

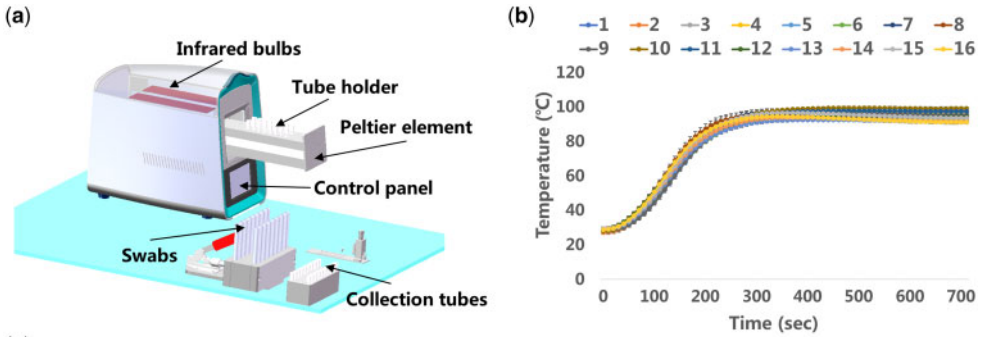

(c)

Inactivation using mode 1 (a.u.)

SARS-CoV-2 Non-inactivation	SARS-CoV-2 Inactivation-56°C, 30 min	SARS-CoV-2 Inactivation-70°C, 12 min	MERS-CoV Non-inactivation	MERS-CoV Inactivation-56°C, 30 min	MERS-CoV Inactivation-70°C, 12 min	Negative control
38855	5	10	2484224	10	5	10
49749	10	5	2451514	10	10	5
38375	5	5	1944031	15	10	5

(d)

Inactivation using mode 2 (a.u.)

MERS-CoV Non-inactivation	MERS-CoV Inactivation-90°C, 5min	MERS-CoV Inactivation-90°C, 12min	MERS-CoV Inactivation-95°C, 5min	MERS-CoV Inactivation-95°C, 12min	MERS-CoV Inactivation-100°C, 5min	MERS-CoV Inactivation-100°C, 12min	Negative control
44574	5	58	0	5	5	5	19
18822	19	53	10	15	5	330	10
17761	10	19	10	15	10	5	19

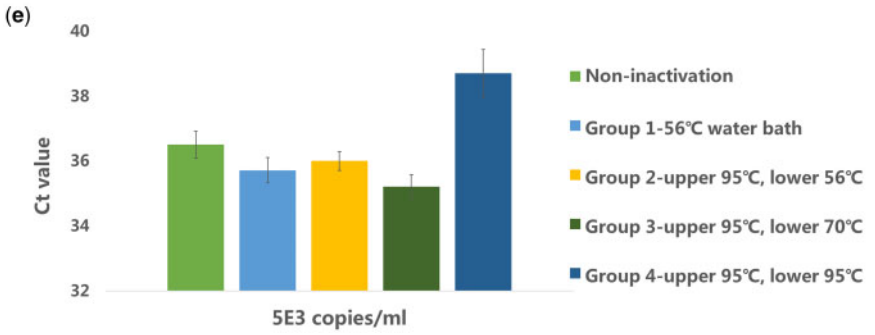

Fig. 3. Pathogen inactivation. (A), Schematic illustration of the pathogen inactivation module, which contains 2 infrared bulbs under the cover, a tube holder that sits 16 collection tubes, a Peltier element attached under the tube holder, and a control panel. (B), Temperature profiles of the upper part of 16 collection tubes by infrared heating. (C), Inactivation of pseudoviruses SARS-CoV-2 and MERS-CoV in preservation buffer using mode 1. (D), Inactivation of pseudovirus MERS-CoV smears in the upper sidewalls and caps using mode 2. In (C) and (D), the negative control refers to cell-plated microwells that do not contain virus samples, and the noninactivated groups refer to cell-plated microwells that contain virus samples that did not go through the inactivation process. The numbers and color codes in the charts represent the magnitude of fluorescent signals in luciferase assay. a.u., arbitrary units. (E), RT-qPCR amplification results of pseudovirus FNV-2019-ncov-abEN at the concentrations of 5E3 copies/mL after inactivation at different conditions ($n = 3$). Noninactivated pseudovirus FNV-2019-ncov-abEN was used as a control to check the integrity of treated nucleic acids. In group 1, the collection tubes containing pseudovirus samples were heated in the water bath at 56 °C for 30 min, whereas in groups 2, 3, and 4, the upper part of tubes was heated at 95 °C while the lower part was heated at 56 °C for 30 min, 70 °C for 12 min, and 95 °C for 12 min, respectively. Ct, threshold cycle.

A possible risk factor for false-negative results by NATs (30, 32, 33) with thermal inactivation of pathogens is compromised nucleic acid integrity due to inappropriate heating. The integrity of heat-inactivated specimen was evaluated using RT-qPCR with pseudovirus FNV-2019-ncov-abEN (Fubio Biological Technology Co., Ltd.). After inactivation, the RNAs of the heat-inactivated samples were released by mixing with sample release reagent (10-μL sample to 10 μL reagent; Sansure Biotech) for 10 min at room temperature. Viral RNAs were quantified by calculating quantification cycle (Cq) values of RT-qPCR using fluorescence probes (Novel Coronavirus [2019-nCoV] Nucleic Acid Diagnostic Kit [Sansure Biotech]; 30 min at 50 °C, 1 min at 95 °C, and 45 cycles of 15 s at 95 °C and 30 s at 60 °C).

PATHOGEN NATS

The microfluidic nucleic acid analyzer is comprises a fully integrated centrifugal microfluidic chip and associated machinery such as spinning and heating modules and the optical detection module. The centrifugal microfluidic chip hosts 2 parallel reactions for analyzing 2 samples simultaneously. Each consists of 3 main modules including nucleic acid extraction, preamplification by reverse-transcription recombinase polymerase amplification, and amplification by LAMP. Inactivated specimen was directly dispensed into the chip by pipetting, and the following liquid-handling and amplification procedures were automatically driven by the centrifugal force to achieve "sample in, answer out"–type NATs of pathogens.

To evaluate the sensitivity of the analyzer, pseudovirus FNV-2019-ncov-abEN was diluted to a wide range of concentration gradients of 100, 150, 300, 1000, 5000, and 10 000 copies/mL and added to the microchip. Repeatability of the analyzer was assessed by testing the pseudovirus FNV-2019-ncov-abEN at the concentration of 1000 copies/mL using 5 batches (6 replicates in each batch) of centrifugal microchips. Robustness of the analyzer was tested by adding a variety of interferents to the pseudovirus FNV-2019-ncov-abEN specimen prepared at the concentration of 150 copies/mL, including azithromycin at 5 mg/L, oseltamivir at 12 mg/L, budesonide at 10 mg/L, meropenem at 100 mg/L, mometasone at 100 mg/L, mucin at 10 mg/L, ceftriaxone at 40 mg/L, tobramycin at 10 mg/L, zanamivir at 10 mg/L, and levofloxacin at 10 mg/L. Final results were processed and reported automatically by the information platform.

SYSTEM EVALUATION

To evaluate the performance of the mobile laboratory in a complete workflow of molecular diagnostics, oropharyngeal swab specimens were collected by the automated robot arm from healthy volunteers, spiked with pseudovirus FNV-2019-ncov-abEN to the concentration of 150 copies/mL, inactivated, and analyzed by the microfluidic nucleic acid analyzer. The control group differed by manual collection of oropharyngeal swab samples ($n = 10$).

CLINICAL EVALUATION OF THE MICROFLUIDIC NUCLEIC ACID ANALYZER

Clinical samples were obtained with informed consent from patients. A total of 736 clinical samples (377 samples from male patients and 359 from female patients; average age: 43.11 years) were collected from 723 patients (370 male patients and 353 female patients; average age: 43.17 years). The diagnostic results of clinical samples using the onboard microfluidic nucleic acid analyzer were compared with those of the reference RT-qPCR method using κ consistency analysis, and the κ coefficient was determined. The diagnostic results of patients using the microfluidic analyzer were also compared with those of the reference standard by clinical assessment.

SUPPORTING SYSTEM

The air ventilation system provided negative pressure at −15 Pa to the whole cabin of the mobile laboratory, and the biosafety level 2 cabinet used a stand-alone air-venting system. Because the sampling window remained open during specimen collection to prevent cross-contamination with the outside environment, a specially designed air curtain was used through which outside air was drawn into the gratings along the sides of the sampling window by negative pressure. Simulation of the air-flow profile in the biosafety cabinet and in close proximity to the sampling window was performed using COMSOL Multiphysics. Details on the stand-alone waterway and power supply systems are given in the online Data Supplement.

Results

MOBILE LABORATORY

In the constructed, van-based mobile laboratory, a 6-axis robot arm with built-in artificial vision and force feedback was used for oropharyngeal swab sampling. The collected specimens were transferred directly to a heating module for rapid inactivation of pathogens, followed by onboard NAT using a fully integrated microfluidic nucleic acid analyzer. The mobile laboratory was equipped with 8 microfluidic nucleic acid analyzers, which appreciably increased the throughput of the mobile laboratory to 150 samples in 8 hours. The onboard information platform possesses a data-driven

pivot capable of real-time and multidimensional perception, surveillance, and intelligent decision-making for response to COVID-19 outbreaks (see online Supplemental Fig. S4).

SPECIMEN COLLECTION

The robot arm demonstrated good repeatability of ±0.1 mm, a small footprint of 128 mm in diameter, and low power consumption of 100 W under typical settings. Movement of the robot arm was precisely controlled, and the status was monitored at multiple checkpoints in a single run, during which autocorrection of the robot arm was applied to ensure safe and seamless operation.

The specimen collection efficiency was evaluated by comparing the Tp values of the *GAPDH* gene in LAMP reactions from human cellular materials of healthy participants that was collected by automated and manual collection (Fig. 2, C). The mean (SD) Tp values of the *GAPDH* gene of automated and manual collections were 13.7 (0.6) min and 14.1 (1.2) min, respectively ($n = 8$). These results showed no significant difference of collected oropharyngeal swab specimens between automated and manual collection.

Fig. 2, D and E, show that the air curtain efficiently takes in air flow from both inside and outside of the biosafety cabinet without noticeable leakage through the sampling window. These results demonstrate successful isolation of the biosafety cabinet from both the outside environment and the laboratory cabin during specimen collection.

PATHOGEN INACTIVATION

As shown in Fig. 3, B, the temperature profiles of the upper part of collection tubes in all positions of the holder demonstrate uniform heating by infrared radiation. It took <5 min to reach the set temperature at 95 °C in the upper part of the collection tubes, with maximum overshooting of <2.0 °C. The SD of stabilized temperatures after heating for 5 min was 2.4 °C.

Figure 3, C, provides data showing that in thermoelectric heating inactivation, the pseudoviruses could be successfully inactivated by heating at both 56 °C for 30 min and 70 °C for 12 min. Fig. 3, D, shows that no viral activity was detected, and the residual viruses left in the upper sidewalls and caps were successfully inactivated. Complete inactivation of the replicable vesicular stomatitis virus can be achieved after infrared heating of the upper part at 95 °C and 97 °C for 12 min (see online Supplemental Fig. S5). Overall, these results demonstrate successful inactivation of pathogens in both solutions and sidewalls within 12 min at the optimized temperature of 95 °C.

Figure 3, F, shows that the Cq values of the RT-qPCR tests of pseudovirus FNV-2019-ncov-abEN increased by >2 when the lower part of the collection tubes was heated at 95 °C compared with other conditions. This result suggests that high-temperature heating in the lower part of the collection tubes damages specimen nucleic acids, leading to substantial loss of detectable nucleic acids in the inactivated samples. In addition, when the temperature of lower part of the collection tubes was <70 °C, the Cq values of inactivated groups remained similar to the control (ΔCq <1), demonstrating the wide applicability of the quick inactivation device to achieve efficient inactivation without causing damage to pathogen nucleic acids.

PATHOGEN NATS

The developed microfluidic nucleic acid analyzer is shown in Fig. 4, A, and the centrifugal disk microfluidic chip is shown in Fig. 4, B. Automated operation brought unprecedented speed; nucleic acid extraction, preamplification, and amplification took <10 min, <15 min, and <20 min, respectively, accounting for a total of <45 min in analysis. Moreover, because of the high sensitivity of the nested isothermal amplification system, preliminary tests with pseudovirus FNV-2019-ncov-abEN frequently produced positive results in as short a time as 35 min. Because all of the nucleic acid amplification operations of inactivated specimens were carried out automatically inside the sealed microchip, physical isolation of operation space as in PCR laboratories was not necessary, greatly alleviating the space restriction of the mobile laboratory.

Performance of the microfluidic nucleic acid analyzer was evaluated in multiple ways. First, the linearity of fluorescent signal detection was tested with FAM (fluorescein amidite) within the concentration range of 0.0625–1.000 μmol/L, and a linearity of 0.9975 was achieved (Fig. 4, D). Second, the sensitivity of the analyzer was evaluated as capable of detecting pseudovirus at a 100% positive detection rate with 20 samples at concentrations of 150 and 300 copies/mL, and showed 90% at the concentration of 100 copies/mL. The limit of detection of the analyzer was thus determined to be 150 copies/mL. Successful detection of both *Open Reading Frame 1ab (ORF1ab)* region and *N* gene suggests robust and unbiased testing of nucleic acids of pathogens. The typical amplification curves of pseudovirus FNV-2019-ncov-abEN at a wide range of different concentrations are demonstrated in Fig. 4, E. Third, the repeatability of the centrifugal microchip was tested by analyzing the Tp values using pseudovirus FNV-2019-ncov-abEN at the concentration of 1000 copies/mL. The analyzed Tp values for *ORF1ab* region and *N* gene of the 30 replicates from 5 batches are shown in Fig. 4,

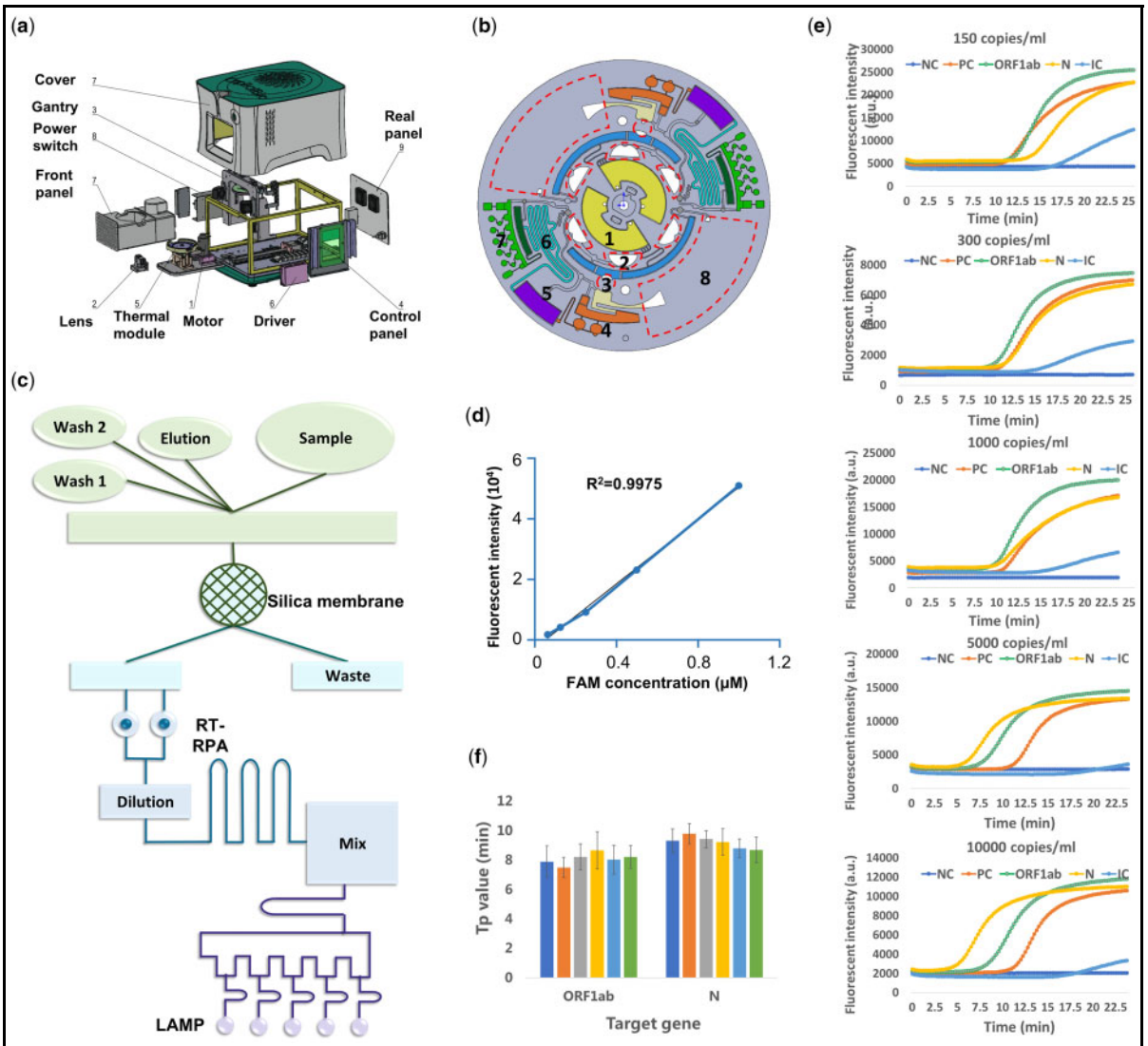

Fig. 4. Microfluidic nucleic acid analyzer. (A), The diagram of the developed microfluidic nucleic acid analyzer. (B), The layout of the fully integrated centrifugal microfluidic chip. The components include (1) sample reservoirs, (2) buffer reservoirs, (3) silica membranes (backside), (4) reverse transcription recombinase polymerase amplification (RT-RPA) reaction chambers, (5) dilution chambers, (6) mixing channels, (7) LAMP reaction chambers, and (8) waste reservoirs. Dried pellets of probes and primers for RT-RPA were directly added to the reaction chambers before packaging. Reagents containing probes and primers for LAMP were prefilled to corresponding chambers at 60 μL and dried at room temperature. (C), The working scheme of the microfluidic nucleic acid analyzer. (D), Linearity of the fluorescent detector using FAM. (E), NAT amplification curves of different concentrations of pseudovirus FNV-2019-ncov-abEN at 150, 300, 1000, 5000, and 10000 copies/mL using the developed analyzer. Positive control (PC): duck plaque virus; negative control (NC): diethyl pyrocarbonate (DEPC)-treated water; internal quality control (IC): GAPDH. (F), Repeatability of Tp values of 5 batches of the centrifugal microchips (6 replicates/batch) by analyzing the *ORF1ab* region and *N* gene of pseudovirus FNV-2019-ncov-abEN at the concentration of 1000 copies/mL. The sequences of the primers used in RT-RPA and LAMP are given in Supplemental Tables S1 and S2.

F. The CVs of the Tp values for the *ORF1ab* region and *N* gene were 11.9% and 8.6%, respectively, demonstrating no significant difference in different batches of NATs. The close Tp values of the *ORF1ab* region and *N* gene show that both of the targeted genes can be detected successfully. Fourth, in clinical samples, various

Table 1. NAT results of collected oropharyngeal swab specimens by the mobile laboratory.

Automated sampling					Manual sampling				
Test	**GAPDH[1]**	**N[1]**	**ORF1ab[1]**	**Detected**	**Test**	**GAPDH[1]**	**N[1]**	**ORF1ab[1]**	**Detected**
CoV0199-B	10.6	10.8	10.4	Y	CoV0199-A	10.4	11	11.4	Y
CoV0214-B	14.8	9	9	Y	CoV0214-A	12.6	11	9.6	Y
CoV0264-B	12.2	11	9.2	Y	CoV0264-A	14	14.6	14.4	Y
CoV0316-B	10	12.8	8.8	Y	CoV0316-A	11.4	11.2	10	Y
CoV0367-B	11.4	8	8	Y	CoV0367-A	12	11.8	10.2	Y
CoV1817-B	12.4	9.4	10.2	Y	CoV1817-A	12.2	11.4	9.6	Y
CoV1823-B	13.6	11.8	7.6	Y	CoV1823-A	13.4	11.8	8	Y
CoV2654-B	12.4	9.8	10.4	Y	CoV2654-A	12.6	9.2	9.4	Y
CoV2656-B	12.8	10.2	8.4	Y	CoV2656-A	13.2	12.2	10.2	Y
CoV2657-B	13.4	11.8	10.4	Y	CoV2657-A	13.4	10.8	9.2	Y
Mean ± SD	12.4 ± 1.4	10.5 ± 1.5	9.2 ± 1.1		Mean ± SD	12.5 ± 1.1	11.5 ± 1.4	10.2 ± 1.7	
Detection rate	10/10	10/10	10/10	10/10	Detection rate	10/10	10/10	10/10	10/10

[1]The numbers of these items represent the Tp values of respective genes in minutes.

interferents may exist in the collected specimen that would inhibit NATs such as those for antiviral drugs, microorganisms, and so forth. In this regard, the Tp values for the *ORF1ab* region and *N* gene of pseudovirus solutions spiked with interferents were close to those without interferents, demonstrating the high specificity of the microfluidic analyzer (see online Supplemental Fig. S6). In particular, even at low concentrations of pseudovirus solutions (e.g., limit of detection of 150 copies/mL), the addition of interferents showed no impact on the detection of target pseudovirus samples. Overall, the microfluidic nucleic acid analyzer demonstrated superior sensitivity, repeatability, and robustness for pathogen NATs, and the compact size and integrated functionality facilitated contamination-free and flexible deployment with the mobile laboratory for on-site diagnostics.

SYSTEM EVALUATION

As shown in Table 1, in all 10 test groups, the specific *ORF1ab* region and *N* gene of the FNV-2019-ncov-abEN virus were reported positive from specimens collected by the robot arm, consistent with the results of manually collected specimens. The mean (SD) of the Tp values of the *GAPDH* gene of specimens from automated and manual collections were 12.4 (1.4) min and 12.5 (1.1) min, respectively, demonstrating successful detection of human genetic materials from oropharyngeal swab specimens. The Tp values for the *ORF1ab* region and *N* gene were very close, demonstrating excellent sensitivity and unbiased detection in pathogenic diagnosis.

EVALUATION WITH CLINICAL SAMPLES

A summary of consistency test results of clinical samples analyzed by the microfluidic nucleic acid analyzer compared with the reference RT-qPCR method is provided in Table 2. Of the 736 clinical samples, 351 samples tested positive and 385 tested negative using the present microfluidic analyzer, compared with 346 positive and 390 negative samples tested by RT-qPCR, showing high positive percentage of agreement of 99.71%, negative percentage of agreement of 98.46%, and overall percentage of agreement of 99.05%, respectively. The 95% CIs for positive, negative and overall percentages of agreement were calculated using the Wilson method (98.38%–99.95%, 96.68%–99.29%, and 98.05%–99.54%, respectively). The κ coefficient of clinical sample evaluation using the microfluidic nucleic acid analyzer and RT-qPCR was determined to be 0.979, showing good consistency of the test results.

Table 2 also shows the consistency test results of patients using the microfluidic analyzer and the reference standard by clinical assessment. Of the 723 patients, 345 tested positive and 378 tested negative using the microfluidic analyzer, compared with 352 positive and 371 negative by the reference standard, showing high sensitivity at 97.73% (95% CI, 95.58%–98.84%), high specificity at 99.73%

Table 2. Summary of evaluation results of clinical COVID-19 samples.

Clinical evaluation			
	RT-qPCR		
Samples	**Positive**	**Negative**	**Total**
Microfluidic analyzer test			
Positive	345	6	351
Negative	1	384	385
Total	346	390	736
	Reference standard		
Patients	**Positive**	**Negative**	**Total**
Microfluidic analyzer test			
Positive	344	1	345
Negative	8	370	378
Total	352	371	723

(95% CI, 98.49%–99.95%), and high overall percentage of agreement at 98.76% (95% CI, 97.65%–99.34%).

Discussion

Infectious disease outbreaks such as the COVID-19 pandemic pose profound challenges worldwide. Limitations of available medical resources and unmet demand of local community-level NAT screening have hindered implementation of timely and effective responses to potential infectious disease outbreaks. The need for mobile laboratories capable of molecular diagnostics applies not only to COVID-19 but to a wide variety of infectious diseases such as viral hemorrhagic fevers including Ebola, Marburg, and Lassa (34–37). Virological evidence has demonstrated that a substantial viral load is present in infected individuals in the early stages of COVID-19 (38–40); therefore, early diagnostics and treatment are the key for outbreak control. The mobile laboratory facilitates rapid and flexible deployment of diagnostic support to disease transmission hotspots such as local communities, airports, and train stations.

The discrete modules of the mobile laboratory have demonstrated superior performance separately and as a whole by successful evaluation with pseudovirus spiked oropharyngeal swab specimens and clinical samples. The mobile laboratory minimized biohazard by using automated specimen collection and inactivation inside the biosafety cabinet and utilizing a fully integrated microfluidic nucleic acid analyzer. Consequently, physical isolation of working areas was not necessary, solving the conflict between biosafety risk management and limited working space onboard. The information platform controls experimental and laboratory information flow and enables every individual mobile laboratory to be a "mobile sentinel" in the infectious disease outbreak, continuously feeding diagnostic results to the real-time monitoring network.

Given regulatory requirements for the van-based mobile laboratory and the limited numbers of patients with COVID-19 in China, testing with clinical samples onboard is currently restricted. However, we completed evaluation of the microfluidic nucleic acid analyzer using 736 clinical samples taken from 723 patients and demonstrated good consistency with RT-qPCR (κ = 0.979). The high efficiency of specimen collection by the robot arm and high sensitivity of the nucleic acid analyzer facilitated highly sensitive testing of oropharyngeal swab specimens, which was demonstrated by the evaluation of combined automated sampling with nucleic acid analysis. In addition, by using the specially designed diaphragm, oropharyngeal swab specimen collection could be readily integrated with the robot arm for establishment of a stable sampling path. This approach significantly improved the safety and comfort of patients as well as the quality of the acquired specimens.

Supplemental Material

Supplemental material is available at *Clinical Chemistry* online.

Nonstandard Abbreviations: COVID-19, coronavirus disease 2019; NAT, nucleic acid–based test; SARS-CoV-2, severe acute respiratory syndrome coronavirus 2; RT-qPCR, reverse transcription quantitative PCR; LAMP, loop-mediated isothermal amplification; Tp, time to positivity; MERS-CoV, Middle East respiratory syndrome coronavirus; Cq, quantification cycle.
Human Gene: *GAPDH*, glyceraldehyde-3-phosphate dehydrogenase

Author Contributions: *All authors confirmed they have contributed to the intellectual content of this paper and have met the following 4 requirements: (a) significant contributions to the conception and design, acquisition of data, or analysis and interpretation of data; (b) drafting or revising the article for intellectual content; (c) final approval of the published article; and (d) agreement to be accountable for all aspects of the article thus ensuring that questions related to the accuracy or integrity of any part of the article are appropriately investigated and resolved.*

W. Xing, J. Wang, C. Zhao, and H. Wang contributed to study design, data analysis, and manuscript drafting. J. Cheng conceived the original idea of the mobile laboratory and, with W. Li, H. Shang, and N. Zhong, co-supervised this work and manuscript drafting. J. Wang, H. Li, D. Wang, Y. Pan, and D. Weng contributed to the development of the robot arm-based specimen collection system. H. Wang, S. Shan, and D. Wang contributed to the quick inactivation device. W. Xing, L. Bai, L. Pan, H.W., Y. Lu, X. Chen, and X. Zhou contributed to the microfluidic nucleic acid analyzer. Z. Zhang and R. Huang contributed to the laboratory information system. C. Zhao, H. Li, J. He, and R. Jin contributed to the design and construction of the vehicle.

Authors' Disclosures or Potential Conflicts of Interest: *Upon manuscript submission, all authors completed the author disclosure form. Disclosures and/or potential conflicts of interest:*

Employment or Leadership: D. Wang, CapitalBio Corp.
Consultant or Advisory Role: None declared.
Stock Ownership: None declared.
Honoraria: D. Wang, CapitalBio Corp.
Research Funding: Guangzhou Institute of Respiratory Health Open Project (Funds provided by China Evergrande Group), Consulting Research Project of the Chinese Academy of Engineering, Emergency Project of the Ministry of Science and Technology of China.
Expert Testimony: None declared.
Patents: C. Zhao, CN211286829U; H. Li, CN211286829U; D. Wang, 2620202048017.X, 26202010261507.X; J. Cheng, CN211286829U.

Role of Sponsor: The funding organizations played no role in the design of study, choice of enrolled patients, review and interpretation of data, preparation of manuscript, or final approval of manuscript.

Acknowledgments: We thank Professor Linqi Zhang at Tsinghua University for providing pseudoviruses and test facility.

References

1. Chu DK, Akl EA, Duda S, Solo K, Yaacoub S, Schünemann HJ, et al. Physical distancing, face masks, and eye protection to prevent person-to-person transmission of SARS-CoV-2 and COVID-19: a systematic review and meta-analysis. Lancet 2020;395:1973–87.
2. Blumenthal D, Fowler EJ, Abrams M, Collins SR. Covid-19–implications for the health care system. N Engl J Med 2020;383:1483–8.
3. Wang C, Horby PW, Hayden FG, Gao GF. A novel coronavirus outbreak of global health concern. Lancet 2020;395:470–3.
4. Hsiang S, Allen D, Annan-Phan S, Bell K, Bolliger I, Chong T, et al. The effect of large-scale anti-contagion policies on the COVID-19 pandemic. Nature 2020;584:262–7.
5. Wu F, Zhao S, Yu B, Chen YM, Wang W, Song ZG, et al. A new coronavirus associated with human respiratory disease in China. Nature 2020;579:265–9.
6. Wolfel R, Corman VM, Guggemos W, Seilmaier M, Zange S, Muller MA, et al. Virological assessment of hospitalized patients with COVID-2019. Nature 2020;581:465–9.
7. Ai T, Yang Z, Hou H, Zhan C, Chen C, Lv W, et al. Correlation of chest CT and RT-PCR testing for coronavirus disease 2019 (COVID-19) in China: a report of 1014 cases. Radiol 2020;296:E32–E40.
8. Yu L, Wu S, Hao X, Dong X, Mao L, Pelechano V, et al. Rapid detection of COVID-19 coronavirus using a reverse transcriptional loop-mediated isothermal amplification (RT-LAMP) diagnostic platform. Clin Chem 2020;66:975–7.
9. Park GS, Ku K, Baek SH, Kim SJ, Kim SI, Kim BT, Maeng JS. Development of reverse transcription loop-mediated isothermal amplification assays targeting severe acute respiratory syndrome coronavirus 2 (SARS-CoV-2). J Mol Diagn 2020;22:729–35.
10. Xia S, Chen X. Single-copy sensitive, field-deployable, and simultaneous dual-gene detection of SARS-CoV-2 RNA via modified RT-RPA. Cell Discov 2020;6:37.
11. Udugama B, Kadhiresan P, Kozlowski HN, Malekjahani A, Osborne M, Li VYC, et al. Diagnosing COVID-19: the disease and tools for detection. ACS Nano 2020;14:3822–35.
12. Ji Y, Ma Z, Peppelenbosch MP, Pan Q. Potential association between COVID-19 mortality and health-care resource availability. Lancet Glob 2020;8:e480.
13. Kavanagh MM, Erondu NA, Tomori O, Dzau VJ, Okiro EA, Maleche A, et al. Access to lifesaving medical resources for African countries: COVID-19 testing and response, ethics, and politics. Lancet 2020;395:1735–8.
14. Grolla A, Jones SM, Fernando L, Strong JE, Stroher U, Moller P, et al. The use of a mobile laboratory unit in support of patient management and epidemiological surveillance during the 2005 Marburg outbreak in Angola. PLOS Negl Trop Dis 2011;5:e1183.
15. Grolla A, Jones S, Kobinger G, Sprecher A, Girard G, Yao M, et al. Flexibility of mobile laboratory unit in support of patient management during the 2007 Ebola-Zaire outbreak in the Democratic Republic of Congo. Zoonoses Public Health 2012;59:151–7.
16. Sugalski G, Murano T, Fox A, Rosania A. Development and use of mobile containment units for the evaluation and treatment of potential Ebola virus disease patients in a United States hospital. Acad Emerg Med 2015;22:616–22.
17. Wölfel R, Stoecker K, Fleischmann E, Gramsamer B, Wagner M, Molkenthin P, et al. Mobile diagnostics in outbreak response, not only for Ebola: a blueprint for a modular and robust field laboratory. Euro Surveill 2015;20:30055.
18. Paweska JT, Jansen van Vuren P, Meier GH, Le Roux C, Conteh OS, Kemp A, et al. South African Ebola diagnostic response in Sierra Leone: a modular high biosafety field laboratory. PLOS Negl Trop Dis 2017;11:e0005665.
19. Weidmann M, Faye O, Faye O, Abd El Wahed A, Patel P, Batejat C, et al. Development of mobile laboratory for viral hemorrhagic fever detection in Africa. J Infect Dis 2018;218:1622–30.
20. Njanpop-Lafourcade BM, Hugonnet S, Djogbe H, Kodjo A, N'Douba AK, Taha MK, et al. Mobile microbiological laboratory support for evaluation of a meningitis epidemic in Northern Benin. PLOS ONE 2013;8:e68401.
21. Zhang Y, Gong Y, Wang CY, Liu WS, Wang ZY, Xia ZP, et al. Rapid deployment of a mobile biosafety level-3 laboratory in Sierra Leone during the 2014 Ebola virus epidemic. PLOS Negl Trop Dis 2017;11:e0005622.
22. Cheng J, Sheldon EL, Wu L, Uribe A, Gerrue LO, Carrino J, et al. Preparation and hybridization analysis of DNA/RNA from *E. coli* on microfabricated bioelectronic chips. Nat Biotechnol 1998;16:541–6.
23. Huang GL, Huang Q, Xie L, Xiang GX, Wang L, Xu H, et al. A rapid, low-cost, and microfluidic chip-based system for parallel identification of multiple pathogens related to clinical pneumonia. Sci Rep 2017;7:6441.
24. Zhang GJ, Zheng GH, Zhang Y, Ma RM, Kang XX. Evaluation of a micro/nanofluidic chip platform for the high-throughput detection of bacteria and their antibiotic resistance genes in post-neurosurgical meningitis. Int J Infect Dis 2018;70:115–20.
25. Liu DC, Zhu YZ, Li N, Lu Y, Cheng J, Xu YC. A portable microfluidic analyzer for integrated bacterial detection using visible loop-mediated amplification. Sens Actuators B Chem 2020;310:127834.

26. Xing WL, Liu YY, Wang HL, Li SL, Lin YP, Chen L, et al. A high-throughput, multi-index isothermal amplification platform for rapid detection of 19 types of common respiratory viruses including SARS-CoV-2. Engineering 2020;6:1130–40.

27. Li SQ, Guo WL, Liu H, Wang T, Zhou YY, Yu T, et al. Clinical application of intelligent oropharyngeal-swab robot: implication for COVID-19 pandemic. Eur Respir J 2020;56:2001912.

28. Gadkar VJ, Goldfarb DM, Gantt S, Tilley PAG. Real-time detection and monitoring of loop mediated amplification (LAMP) reaction using self-quenching and dequenching fluorogenic probes. Sci Rep 2018;8:5548.

29. World Health Organization. Laboratory biosafety guidance related to coronavirus disease (COVID-19): interim guidance, 19 March 2020. Geneva (Switzerland): World Health Organization; 2020.

30. Pastorino B, Touret F, Gilles M, Luciani L, de Lamballerie X, Charrel RN. Evaluation of heating and chemical protocols for inactivating SARS-CoV-2. Viruses 2020;12:624.

31. Ju B, Zhang Q, Ge J, Wang R, Sun J, Ge X, et al. Human neutralizing antibodies elicited by SARS-CoV-2 infection. Nature 2020;584:115–9.

32. Leclercq I, Batejat C, Burguiere AM, Manuguerra JC. Heat inactivation of the Middle East respiratory syndrome coronavirus. Influenza Other Respir Viruses 2014;8:585–6.

33. Pan Y, Long L, Zhang D, Yuan T, Cui S, Yang P, et al. Potential false-negative nucleic acid testing results for severe acute respiratory syndrome coronavirus 2 from thermal inactivation of samples with low viral loads. Clin Chem 2020;66:794–801.

34. Vetter P, Kaiser L, Schibler M, Ciglenecki I, Bausch DG. Sequelae of Ebola virus disease: the emergency within the emergency. Lancet Infect Dis 2016;16:e82–e91.

35. Rojek A, Horby P, Dunning J. Insights from clinical research completed during the West Africa Ebola virus disease epidemic. Lancet Infect Dis 2017;17:E280–92.

36. Zhang XN, Tan Y, Ling Y, Lu G, Liu F, Yi ZG, et al. Viral and host factors related to the clinical outcome of COVID-19. Nature 2020;583:437–40.

37. Verity R, Okell LC, Dorigatti I, Winskill P, Whittaker C, Imai N, et al. Estimates of the severity of coronavirus disease 2019: a model-based analysis. Lancet Infect Dis 2020;20:669–77.

38. Wyllie AL, Fournier J, Casanovas-Massana A, Campbell M, Tokuyama M, Vijayakumar P, et al. Saliva or nasopharyngeal swab specimens for detection of SARS-CoV-2. N Engl J Med 2020;383:1283–6.

39. Pan Y, Zhang D, Yang P, Poon LLM, Wang Q. Viral load of SARS-CoV-2 in clinical samples. Lancet Infect Dis 2020;20:411–2.

40. To KK, Tsang OT, Leung WS, Tam AR, Wu TC, Lung DC, et al. Temporal profiles of viral load in posterior oropharyngeal saliva samples and serum antibody responses during infection by SARS-CoV-2: an observational cohort study. Lancet Infect Dis 2020;20:565–74.